

# Spoofing of Quantum Channels Enables Low-Rank Projective Simulation

Timothy Heightman<sup>1,2</sup> and Grzegorz Rajchel-Mieldzióć<sup>3,1</sup>

<sup>1</sup>ICFO - Institut de Ciències Fòniques, The Barcelona Institute of Science and Technology, 08860 Castelldefels (Barcelona), Spain

<sup>2</sup>Quside Technologies SL, Carrer d'Esteve Terradas, 1, 08860 Castelldefels, Barcelona, Spain

<sup>3</sup>BEIT, ul. Mogilska 43, 31-545 Kraków, Poland

The ability to characterise and discern quantum channels is a crucial aspect of noisy quantum technologies. In this work, we explore the problem of distinguishing quantum channels when limited to sub-exponential resources, framed as von Neumann (projective) measurements. We completely characterise equivalence classes of quantum channels with different Kraus ranks that have the same marginal distributions under compatible projective measurements. In doing so, we explicitly identify gauge freedoms which can be varied without changing those compatible marginal outcome distributions, opening new avenues for quantum channel simulation, variational quantum channels, as well as novel adversarial strategies in noisy quantum device certification. Specifically, we show how a Sinkhorn-like algorithm enables us to find the minimum admissible Kraus rank that generates the correct outcome marginals. For a generic  $d$ -dimensional quantum system, this lowers the Kraus rank from  $d^2$  to the theoretical minimum of  $d$ . For up to  $d = 20$ , we numerically demonstrate our findings, for which the code is available and open source. Finally, we provide an analytic algorithm for the special case of spoofing Pauli channels.

## 1 Introduction

In the era of noisy intermediate-scale quantum (NISQ) devices, we may characterise quantum hardware by studying the time evolution of quantum states. Whilst closed quantum systems undergo unitary evolution, current quantum hardware contains non-unitary processes; either by design through readout, or through noise encountered in a given device. Recent attention has been given to constructing quantum hardware capable of executing unitary dynamics, with quantum error correction codes getting ever-closer to their goal of practical quantum advantage [1–4].

On the other hand, much success has been found in error *mitigation* in quantum hardware [5–7], defined as the act of better understanding the true open quantum dynamics of a many-body system with the goal of facilitating improved optimal control and readout. The mathematical language to study open quantum systems is quantum channels, with

---

Timothy Heightman: [theightman@icfo.eu](mailto:theightman@icfo.eu)

Grzegorz Rajchel-Mieldzióć: [grzegorzrajchel@gmail.com](mailto:grzegorzrajchel@gmail.com),

Both authors contributed equally to this article.

the number of degrees of freedom scaling exponentially in the number of subsystems [8]. This curse of dimensionality makes it difficult for those who wish to better understand, characterise, or simulate open quantum many-body dynamics [9–16]. Finding accurate models for such systems is known to be hard in general [17].

Recent attention has thus been given to tackling this problem by introducing low-dimensional representations [18, 19] or approximations [20, 21] to quantum channels. In this contribution, we argue the equivalence of characterising quantum channels for many bodies with sub-exponential resources and characterising channels of a smaller number of bodies with a limited set of projective measurements, defined as rank-one von Neumann measurements [22]. They can frame sub-exponential resources because they form a subset of the number of axes of a given many-body Hilbert space. This situation is analogous to using informationally complete positive-operator valued measures (IC-POVMs), but with a sub-exponential number of shots, as characterising channels requires exponential resources [23]. Therefore, in the absence of exponential resources, we cannot perform an entire IC-POVM without introducing significant classical uncertainty. Consequently, IC-POVMs with a sub-exponential number of shots are effectively informationally incomplete when it comes to channel distinguishability.

It is this fact that gives rise to gauge freedoms which create equivalence classes within the space of quantum channels. Importantly, these equivalence classes contain a range of different Kraus ranks. As such, we can vary these gauges to change the Kraus rank of a channel without affecting the distributions of results from projective measurements. Further justification comes from the fact that distinguishing quantum channels is QIP-hard [24]. We therefore should be able to perform some changes to a quantum channel which can go undetected by the user of this channel when they have access to sub-exponential resources. Our findings show that we can perform these changes in such a way that the output marginal distributions under the set of observables remain *identical*. We refer to this as *spoofing* a given channel with a different channel, when given access to sub-exponential resources to distinguish them. From a simulation perspective, this allows us to create a low-rank simulation of a given channel which is exact over a subset of its marginal distributions, giving a quadratic reduction in the rank and therefore, hardness of the simulability. Operationally, this opens avenues for adversarial settings whereby one can spoof a channel with one of lower Kraus rank, without being detected – cheating users of quantum hardware out of their resource-expensive channels.

One might argue that randomized measurement setups like classical shadows [25, 26] can defend against this adversarial strategy. However, even in this setting, one may only detect the spoofers described in this contribution with some success probability. This is because whilst these measurements are *technically* informationally complete, to know these distributions to a reasonable error still requires exponential resources. More concretely, we will see that a  $d$ -dimensional quantum channel with a randomised measurement strategy of  $M$  shots would detect changes to the original  $d$ -dimensional channel with probability  $p \sim \mathcal{O}(M/\epsilon d^2)$ , up to a precision  $\epsilon$ . Furthermore, every architecture which can realise a randomized measurement requires a local unitary rotation which will introduce additional noise to the system.

To summarize, if the measurement of the output state is not informationally complete, the spoofing can always be exploited. In order to avoid spoofing entirely, it is therefore necessary to measure in a precise manner, requiring an exponentially large number of shots. This provides lower bounds on the necessary resources for full security when it comes to device certification. Consequently, it is necessary to take into account these spoofing families defined by equivalence classes to prevent adversarial strategies and certify the

security of quantum devices. It is also advantageous to exploit these spoofing families to find optimal strategies for low-rank simulation of quantum channels which are *exact* in the marginals of projective measurements.

The rest of this paper is structured as follows. We begin by recalling some basic properties of quantum channels in Section 2, and formally define the quantum channel spoofing problem in Section 3. In Section 4, we detail how this problem gives rise to two types of spoofing, each with different physical interpretations. Later on, in Section 5, we explore an important example of how these gauge freedoms can be used to change the rank of Pauli channels, providing geometric insights to the origins of these gauge freedoms. Section 6 then offers a more extended discussion on the significance of this contribution for adversarial strategies in quantum device certification, quantum simulation, and variational quantum algorithms based on channels [27]. In lieu of this discussion, we provide a numerical demonstration for finding the channel of minimal Kraus rank in a given spoofing equivalence class for a generic  $d$ -dimensional channel in Section 7. We also provide an analytic algorithm for identifying the minimal Kraus rank channel in a given spoofing equivalence class for the special case of Pauli channels, formalising the examples given in Section 5. Finally, we offer some concluding remarks and open problems that arise from our contribution in Section 8.

## 1.1 Related works

The main practical result of the present work concerns simulation of a channel with a different channel of lower Kraus rank such that the compatible marginals remain identical. This is important from the experimental perspective, as the dimension of the ancilla is equal to the Kraus rank. Recently, Lancien and Winter [20] have constructed a protocol to simulate a quantum channel with a different channel of lower rank. Their simulating channel is considered successful if *all* marginal distributions that arise from it are  $\epsilon$ -close to the true distribution, using Schatten  $p$ -Norms as their measure of closeness. Whereas in Ref. [28], the authors are able to simulate high-dimensional quantum measurements by exploiting the incompatibility of measurement operators which form an informationally complete cover of the space. In doing so, an observer would not be able to tell the difference between the simulated and true measurements since they would need access to marginals corresponding to incompatible observables in order to distinguish between the two. Our work takes the philosophy behind Ref. [28], and extends it to the more general case of quantum channels. This provides a framework in which one can provide a simulation of a quantum channel whose accuracy is exact when looking at compatible marginal distributions. In other words, our framework enables the simulation of quantum channels with lower-rank ones which are exact in the compatible marginals, differing only in the marginals of observables whose measurements cannot be simultaneously obtained.

Very recently, a couple of preprints were posted exploring similar topics of channel simulation. Refs. [29–31] discuss the possibility of simulating a channel with a cheaper one that is close to the original one up to some error. These approaches differ from our setup in a sense that spoofing is not detectable even in the limit of infinite number of measurements when restricted to a single basis.

## 2 Quantum Channel Representations

Recall that a quantum channel  $\mathcal{E} : B(\mathcal{H}) \rightarrow B(\mathcal{H})$  is represented as a Completely Positive Trace Preserving (CPTP) map on the space of operators,  $B(\mathcal{H})$ , of a Hilbert space  $\mathcal{H}$ .

Representing the action of CPTP maps can be done in several equivalent ways. First, one may characterise a channel by its action on an input density matrix,  $\rho$ , as

$$\mathcal{E}(\rho) = \sum_{r=0}^R K_r \rho K_r^\dagger, \quad (1)$$

where the operators  $K_r$  are the so-called Kraus operators acting on the density matrix by left- and right-matrix multiplication. Unlike unitary dynamics, these operators need only satisfy  $\sum_{r=0}^R K_r K_r^\dagger = \mathbb{1}$  in order for the map to be trace-preserving. We note a well-established fact that such a representation is not unique [32], and several sets of Kraus operators can represent the same quantum channel via the so-called unitary mixing gauge freedom. Such a transformation does *not* change the action of the channel, but only its representation. We therefore recall the definition of the *Kraus rank* as the minimum number of Kraus operators needed to represent the channel action.

An alternative representation of a channel  $\mathcal{E}$  is the Choi matrix  $J_{\mathcal{E}}$ , defined as

$$J_{\mathcal{E}} = (\mathbb{1}_d \otimes \mathcal{E}) |\Omega\rangle \langle \Omega|, \quad (2)$$

where  $|\Omega\rangle = \frac{1}{\sqrt{d}} \sum_{i=0}^{d-1} |i i\rangle$  is the normalised, maximally entangled state in  $\mathcal{H}_d \otimes \mathcal{H}_d$ . The relationship between the Choi and the Kraus representation is given via the spectral theorem. As a consequence, the rank of the Choi matrix is equal to the Kraus rank of the channel [32]. Since a quantum channel is a CPTP map, its Choi matrix is Hermitian and the partial trace of this Choi matrix over the second subsystem is an identity matrix of size  $d$

$$\text{Tr}_B (J_{\mathcal{E}'}) = \mathbb{1}. \quad (3)$$

Additionally, we recall another description of a channel via its natural (superoperator) representation. This formulates the action of a channel as a linear operation in the pseudo-vector space of quantum mixed states<sup>1</sup>. To do so, we vectorize a quantum state  $\rho \rightarrow \vec{\rho}$  row by row; then, the channel  $\mathcal{E}$  acts as superoperator  $S$

$$S \vec{\rho} = S_{ijkl} \rho_{kl}. \quad (4)$$

To obtain the output state  $\mathcal{E}(\rho)$ , one needs to “devectorize” the state  $S \vec{\rho}$ . Operator  $S$  can be thought of as a matrix of order  $d^2$  or as a tensor  $S_{ijkl}$ , with each index taking on  $d$  values. The natural representation can be obtained from Kraus matrices  $\{K_m\}_m$  through  $S = \sum_m K_m \otimes K_m^*$  or from the Choi  $C$  matrix via reshuffling  $S = C^R$  [32] (see App. A for more detail).

We will use these three representations interchangeably throughout the rest of this manuscript. The choice of which to use is made simply for calculational ease and conceptual clarity. For the convenience of the reader, we summarise the relationships between the equivalent representations in Fig. 1.

Finally, we note a convenient equivalent reindexing for Choi and natural representations known as *double index* notation. This is a way of indexing a  $d^2 \times d^2$  matrix  $M_{\mu\nu}$ , where  $\mu, \nu \in \{1, \dots, d^2\}$ , in terms of four indices,

$$M_{\mu\nu} \rightarrow M_{ijkl}, \quad (5)$$

where  $\mu \rightarrow i, j \in \{1, \dots, d\}$ , s.t.  $i = id + b$  and  $\nu \rightarrow k, l \in \{1, \dots, d\}$  s.t.  $\nu = kd + l$ . The advantage of this re-indexing is that it takes into account the tensor-product structure of super-operators. We will also make use of this re-indexing technique throughout the manuscript.

---

<sup>1</sup>This is not a proper vector space since not all linear combinations of states form a valid quantum state.

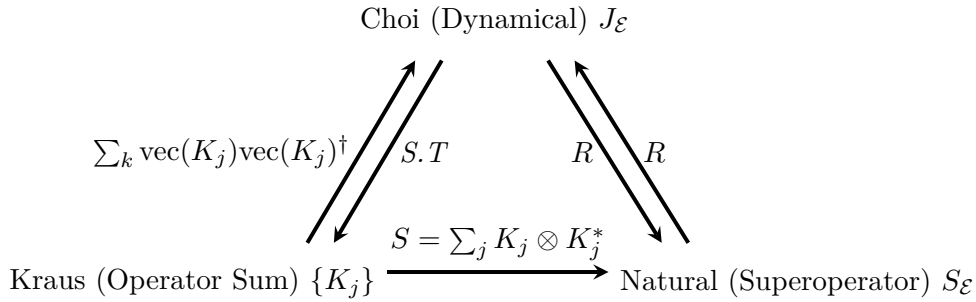


Figure 1: The equivalent representations of a quantum channel,  $\mathcal{E}(\rho) = \sum_j K_j \rho K_j^\dagger$ , where  $\{K_j\}$  are the so-called Kraus operators. Here, by  $S.R$  we refer to the Spectral Theorem [32], i.e., the procedure of computing the eigenvectors of the Choi matrix, and converting them to matrices via the inverse procedure of vectorisation. By  $R$ , we mean the reshuffling operation, explained in detail in App. A. We refer the reader to [32] for a more detailed account of the Choi-Jamiołkowski isomorphism and the representation theory that underpins this info-graphic.

### 3 The Quantum Channel Spoofing Problem

Consider a channel acting on the space of  $d$ -dimensional operators,  $\mathcal{E} : B(\mathcal{H}_d) \rightarrow B(\mathcal{H}_d)$  with Choi matrix  $J_{\mathcal{E}}$ . We seek a secondary, different map,  $\mathcal{E}' : B(\mathcal{H}_D) \rightarrow B(\mathcal{H}_D)$  such that the probability of observing compatible outcomes on both channels are the same. The rationale for our choice stems from the fact that all measurements in a laboratory are done via projective measurements. Those are defined via orthonormal bases; here, we focus on one of them.

We consider the scenario where this basis is the only accessible one for measurements. However, it is possible to repeat them as many times as necessary thus obtaining the infinite, accurate statistics. The rest of the paper is devoted to study the implications that this restriction generates on the set of channels, as argued in the introduction. We are ready to pose the central problem of this contribution.

*Given a quantum channel  $\mathcal{E}$ , and a set of projective measurements,  $\mathcal{M}$ , does there exist a channel  $\mathcal{E}'$  whose Choi matrix,  $J_{\mathcal{E}} \neq J_{\mathcal{E}'}$  such that the marginal distributions of  $\mathcal{M}$  remain unchanged?*

In more mathematical terms, we consider outcomes specified by POVM set  $\mathcal{M} = \{|q\rangle\langle q|\}_{q=0}^{d-1}$ , with operators corresponding to computational basis measurements<sup>2</sup>. We thus require that

$$p_{\mathcal{M}}(q|\mathcal{E}(\rho)) = p_{\mathcal{M}}(q|\mathcal{E}'(\rho)), \quad \forall |q\rangle\langle q| \in \mathcal{M}, \quad \rho \in B(\mathcal{H}), \quad (6)$$

which defines an equivalence relation

$$\mathcal{E} \sim_{\mathcal{M}} \mathcal{E}', \quad (7)$$

between channels  $\mathcal{E}$  and  $\mathcal{E}'$ . Note here that since the measurement set is not informationally complete, not all characteristics of an output state can be gathered. In particular, by measuring in a fixed basis we obtain diagonal elements of the output state in the basis of the projector.

---

<sup>2</sup>In principle the problem is well-defined for any projective measurements as these are the same as the computational basis up to a unitary rotation.

Alternatively, instead of considering the indistinguishability of all the measurements in a single basis, we could focus on the description of the evolution of the observables. This is done via means of the adjoint map<sup>3</sup>  $\mathcal{E}^\dagger$  to the original channel  $\mathcal{E}$ , which is defined as the unique linear map that satisfies

$$\langle \mathcal{E}^\dagger(\rho), \sigma \rangle = \langle \rho, \mathcal{E}(\sigma) \rangle, \quad (8)$$

for all density matrices  $\rho$  and  $\sigma$ . For us, however, the adjoint map is interesting because it allows for the evolution of the observables rather than the states.

We consider two channels  $\mathcal{E} \neq \mathcal{E}'$ , to be different when their Choi matrices,

$$J_{\mathcal{E}} \neq J_{\mathcal{E}'}, \quad (9)$$

are not the same, as several Kraus representations may have the same channel action [32]. To summarise, we seek to classify the sets of quantum channels satisfying  $p_{\mathcal{M}}(q|\mathcal{E}(\rho)) = p_{\mathcal{M}}(q|\mathcal{E}'(\rho))$  for any input state  $\rho$  with computational basis measurements. For the rest of the paper, we assume that  $\mathcal{M}$  is defined through the computational basis. We provide an explicit statement of the main problem in terms of Kraus representation in App. B.

## 4 Parametrization of Spoofing Channels

In this section, we explain how the problem defined in Sec. 3 gives rise to two distinct classes of spoofer shown in Fig. 2, hereby referred to as Type-I and Type-II. The key intuition behind there being two classes is that quantum channels are not always reversible (by construction). So, if we have a pair of channels such that  $J_{\mathcal{E}'} \neq J_{\mathcal{E}}$ , we cannot guarantee that

$$J_{\mathcal{E}'} = \Phi \circ J_{\mathcal{E}}, \quad (10)$$

since this would require the inverse  $\Phi = J_{\mathcal{E}'} \circ J_{\mathcal{E}}^{-1}$  to always be a valid channel. This is not the case in general for non-unitary processes, where  $J_{\mathcal{E}}^{-1}$  is not necessarily a valid channel. Formally, the structure and distinction between Type-I and Type-II spoofers comes from the fact that quantum dynamics is not strictly bi-divisible [33, 34].

In Type-I spoofing, we consider the scenario where we have a (possibly unknown) channel  $\mathcal{E}$ , whose marginals of projective measurements can equivalently be obtained from a divisible channel  $\mathcal{E}' = \Phi \circ \mathcal{E}$ . On the other hand, Type-II spoofing seeks to replace a given (and known) channel,  $\mathcal{E}$ , with a new channel  $\mathcal{E}'$ , which is not necessarily divisible. While this difference may be subtle, we see a profound difference in the number gauge freedoms that each type allows, as well as their use-cases in adversarial settings, efficient quantum channel simulation, and variational quantum algorithms. See Sec. 6 for further discussion.

We now seek to understand the structure of the spoofing channels for Type-I and Type-II by characterizing their gauge degrees of freedom. Here, by a gauge we mean the freedom to vary the value of parameters of the channel without changing the marginal distribution in line with Sec. 3.

### 4.1 Type-I Spoofing

In accordance with Fig. 2, let the original channel be denoted  $\mathcal{E}$ , and the spoofing channel,  $\mathcal{E}'$ , be the result of concatenating  $\mathcal{E}$  with some other channel  $\Phi$ . That is,

$$\mathcal{E}' = \Phi \circ \mathcal{E}. \quad (11)$$

---

<sup>3</sup>Notably, the adjoint map is not necessarily a quantum channel, as it can map states to non-physical states.

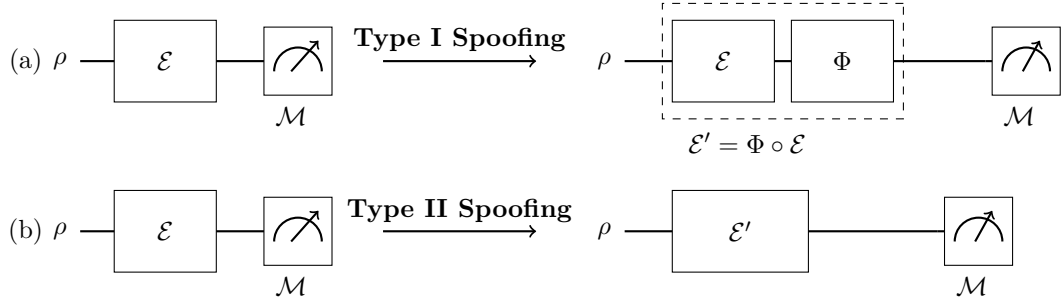


Figure 2: Two inequivalent types of spoofing referred to as Type-I Spoofing (a), and Type-II Spoofing (b). In Type-I Spoofing, we assume we have access to the output of a given channel  $\mathcal{E}$  and are able to concatenate a spoofing channel  $\Phi$  to it, such that the resultant channel,  $\mathcal{E}' = \Phi \circ \mathcal{E}$  is divisible into these two constituent parts. The resultant channel in (a) is depicted inside the dashed line. In Type-II Spoofing, we assume no such access to  $\mathcal{E}$ . Here, the spoofing channel is not necessarily divisible.

The natural representation,  $S_\Phi$  must act as the identity channel,  $S_{\mathbb{1}}$ , over all measurable components of  $\rho$ . As such, the gauges in  $S_\Phi$  form bounded variables along its diagonal, each with modulus smaller than one.

**Theorem 1.** *The natural representation of the Type-I spoofing channel,  $S_\Phi$ , is a diagonal matrix.*

*Proof.* In the basis of the measurement set, we require the diagonal of the output density matrix to be the same when applying  $\mathcal{E}$  or  $\mathcal{E}'$  in order to generate the same marginals. Thus,  $S_\Phi$  must not cause changes to  $\mathcal{E}$  on entries which will affect observable components of the density matrix. When applied to a state,  $\rho$ , in vectorised form (as per the left-hand side of Eq. (4)), this constrains some rows of  $S_\Omega$ . In particular, the rows that act on observable parts of  $\rho$  must be the same as the identity matrix. On other rows however,  $S_\Omega$  is free to vary, implying the following block structure,

$$S_\Phi = \begin{pmatrix} 1 & \dots & 0 & \dots & 0 \\ \boxed{(d+1) \times d^2} \\ 0 & \dots & 1 & \dots & 0 \\ \boxed{\ddots} \\ 0 & \dots & 0 & \dots & 1 \end{pmatrix}, \quad (12)$$

where the rectangular blocks correspond to free sub-matrices of size  $(d+1) \times d^2$ . The form of each block stems from the way in which a density matrix is vectorised; these blocks act on the components of  $\vec{\rho}$  which correspond to off-diagonal terms in the matrix representation decomposed in the basis of our compatible measurements.

We also require that  $\Phi$  is a CPTP map, adding constraints for trace preservation, and a Hermitian output. These conditions are simpler to establish by switching to the Choi representation, since the channel is CPTP if and only if its Choi matrix is positive semi-definite [32]. In the Choi representation, we may enforce this via principal minors (Sylvester's criterion). Applying Sylvester's criterion to  $J_\Phi = (S_\Phi)^R$ , we find that the only remaining free parameters are those that lie on the diagonal in the natural representation,  $S_{ab}$ . That is, the set of elements  $\{S_{22}, \dots, S_{d^2-1, d^2-1}\}$  corresponds to gauge freedoms of the channel in the natural representation

$$S_\Phi = \text{diag}(1, a_1, \dots, a_d, 1, a_{d+1}, \dots, a_{d^2-d}, 1). \quad (13)$$

□

In order to enforce trace preservation, the above gauge degrees of freedom must be bounded with modulus less than one,  $|a_i| \leq 1$ , while the Hermiticity of the Choi matrix provides the last condition on certain elements  $a_i = a_j^*$ . This leads to the following corollary.

**Corollary 2.** *The number of free real parameters of Type-I spoofing equivalence class of a channel on  $d$ -dimensional states is  $d^2 - d$ .*

*Proof.* There are  $d^2 - d$  complex parameters that stem from Eq. (13). The trace-preserving condition does not lower the dimensionality of the equivalence class but only restricts its accessible values. However, the Hermiticity constraint on the Choi matrix adds  $d^2 - d$  conditions on complex parameters  $a_i$ s, which concludes the proof. □

We end the subsection with a characterisation of the Type-I spoofing equivalence family for 1-qubit channels.

**Example 3.** *In Type-I spoofing, the gauge freedoms for an arbitrary 1-qubit channel consist of a single complex parameter,  $a \in \mathbb{C}$ , in the Choi representation of channel  $\Phi$  from Eq. (11) (see also Fig. 2)*

$$J_\Phi = \begin{pmatrix} 1 & 0 & 0 & a \\ 0 & 0 & 0 & 0 \\ 0 & 0 & 0 & 0 \\ a^* & 0 & 0 & 1 \end{pmatrix}. \quad (14)$$

## 4.2 Type-II Spoofing

Consider the scenario in which the simulation of  $\mathcal{E}$  is done by an entirely different channel. We therefore seek a new channel  $\mathcal{E}'$  such that its action alone on any input state produces the same marginals as  $\mathcal{E}$  with respect to the compatible measurement set  $\mathcal{M}$ , i.e., satisfying Eq. (6). We note that Type-II spoofing needs prior knowledge of the given channel, but can be constructed for any given input channel.

**Theorem 4.** *Consider the Type-II spoofing equivalence class of a  $d$ -dimensional channel  $\mathcal{E}$  (Fig. 2). Then, a channel  $\mathcal{E}'$  belongs to the equivalence class defined by Eqs. (6) and (7) if and only if its Choi matrix  $J_{\mathcal{E}'}$  has the following structure:*

1. *the diagonal blocks of size  $d \times d$  of  $J_{\mathcal{E}'}$  must be equal to the diagonal blocks of  $J_{\mathcal{E}}$ ,*
2.  *$J_{\mathcal{E}'}$  is Hermitian and positive semi-definite  $J_{\mathcal{E}'} \geq 0$ ,*
3. *its partial trace (see Eq. 2) is an identity matrix,  $\text{Tr}_B(J_{\mathcal{E}'}) = \mathbb{1}$ .*

*Proof.* The points (2) and (3) must hold for any valid channel  $\mathcal{E}'$ , so it remains to prove the equivalence of (1) with Type-II spoofing. We begin with an observation concerning the natural representation: if  $\mathcal{E}'$  belongs to the same spoofing equivalence class as the original channel  $\mathcal{E}$ , then for every input state  $\rho$ , the output states for  $\mathcal{E}$  and  $\mathcal{E}'$  must agree in the diagonal elements,

$$\forall q: \langle q | \mathcal{E}(\rho) | q \rangle = \langle q | \mathcal{E}'(\rho) | q \rangle. \quad (15)$$

This means that in the natural (superoperator) representation, the two vectors  $S_{\mathcal{E}} \vec{\rho}$  and  $S_{\mathcal{E}'} \vec{\rho}$ , agree on the elements which correspond to diagonal elements of output density matrices. Using double index notation from Eq. (5), this means that when  $i = j$ ,

$$[S_{\mathcal{E}} \vec{\rho}]_{ij,kl} = [S_{\mathcal{E}'} \vec{\rho}]_{ij,kl} \quad \forall k, l. \quad (16)$$



Since this must be true for all input states,  $\rho$ , the equality must hold at the level of  $S_{\mathcal{E}}$  on the appropriate rows. That is,

$$\forall k, l: [S_{\mathcal{E}}]_{ij,kl} = [S_{\mathcal{E}'}]_{ij,kl}, \quad (17)$$

when  $i = j$ . To obtain the Choi matrix of both channels, we may apply reshuffling (see Fig. 1 and App. A), yielding

$$\forall j, l: [J_{\mathcal{E}}]_{ij,kl} = [J_{\mathcal{E}'}]_{ij,kl} \quad (18)$$

when  $i = k$ , which is exactly the condition for equality of the diagonal blocks. Observe that whenever  $i \neq k$ , the only requirements for blocks stem from conditions (2) and (3).

For the converse direction, we must prove that if all the diagonal blocks of the Choi matrices are equal, then the channels belong to the same Type-II equivalence class,  $\mathcal{E} \sim_{\mathcal{M}} \mathcal{E}'$ . The equality of diagonal blocks of the Choi matrices lead to the equality of rows of the natural representations that correspond to Eq. (16). From this follows that for any input state the diagonal part of the output density matrix is equal independently on the used channel,  $\mathcal{E}$  or  $\mathcal{E}'$ . This proves the equivalence in both directions.  $\square$

Intuitively, condition (1) of Thm. 4 means that the Choi matrix of  $\mathcal{E}'$  is of the form

$$J_{\mathcal{E}'} = \begin{pmatrix} \boxed{d \times d} & \circ & \circ & \circ & \circ & \dots \\ \circ & \circ & \boxed{d \times d} & \circ & \circ & \dots \\ \circ & \circ & \circ & \circ & \boxed{d \times d} & \dots \\ \circ & \circ & \circ & \circ & \circ & \dots \\ \circ & \circ & \circ & \circ & \circ & \dots \\ \vdots & \vdots & \vdots & \vdots & \vdots & \ddots \end{pmatrix}, \quad (19)$$

where the boxes are of size  $d \times d$  and are constrained to take the same values as the Choi matrix of the original channel,  $J_{\mathcal{E}}$ . It is for this reason that  $\mathcal{E}$  must be known by a Type-II spoofer; the  $d \times d$  are explicitly dependent on  $J_{\mathcal{E}}$ . The rest of the elements, denoted by dots  $\circ$ , are free to vary provided they satisfy conditions (2) and (3). This leads to the following corollary.

**Corollary 5.** *The number of free real parameters of the Type-II spoofing equivalence class of a channel on  $d$ -dimensional states is  $d^4 - d^3 - d^2 + d$ .*

*Proof.* The proof is based on the counting of the constraints. First, observe that a  $d$ -dimensional quantum channel admits a Choi matrix representation of *a priori*  $d^4$  complex elements. The Hermiticity of the Choi matrix leaves  $d^4$  real parameters. Next, its partial trace must satisfy, Eq. (3), introducing  $d^2$  constraints.

We then introduce the constraints arising from the  $d \times d$  diagonal blocks which must remain the same in both  $J_{\mathcal{E}}$  and  $J_{\mathcal{E}'}$ . Since there are  $d$  copies of these blocks, we would naively assume that this introduces a further  $d^3$  constraints. However, we would then be over-counting the Hermiticity constraint, as these  $d$  sub-blocks are themselves Hermitian. Therefore, keeping these blocks identical and Hermitian presents  $d^3 - d$  constraints. Combining the above, we see that the number of free real parameters is  $d^4 - d^3 - d^2 + d$ .  $\square$

**Example 6.** *In the simplest example of one-qubit case, the spoofing freedom for a channel consists of 3 complex (6 real) parameters in the Choi representation*

$$\left( \begin{array}{cc|cc} \boxed{\phantom{00}} & a & b & \\ \hline & c & -a & \\ a^* & c^* & & \\ \hline b^* & -a^* & \boxed{\phantom{00}} & \end{array} \right), \quad (20)$$

where two empty boxes contain the elements of  $2 \times 2$  diagonal blocks, whose values are determined by the original Choi matrix  $J_{\mathcal{E}}$ .

Lastly, let us remark that using the adjoint map allows for an alternative description of the spoofing freedom. Namely, for all the channels,  $\mathcal{E}'$ , in a given Type-II spoofing equivalence class, the adjoint maps  $\mathcal{E}'^\dagger$  will agree on the computational basis states, i.e.,

$$\mathcal{E} \sim_{\mathcal{M}} \mathcal{E}' \iff \forall i: \mathcal{E}'^\dagger(|i\rangle\langle i|) = \mathcal{E}^\dagger(|i\rangle\langle i|). \quad (21)$$

The above conditions means that the diagonal blocks of the Choi matrices of the adjoint maps also agree, in strict analogy to condition (1) from Theorem. 4.

## 5 Case study: Pauli Channels and the Computational Basis

In this section, we show how to identify the gauge freedoms from Sec. 4 for Pauli channels, defined in the Kraus representation as,

$$\mathcal{E}(\rho) = \sum_j \alpha_j P_j \rho P_j^\dagger, \quad (22)$$

where  $P_j \in \mathcal{P}_N$  is a member of the Pauli group on  $N$  qubits. We choose the computational basis as our example of the projective measurement set as an instructive example. This is because any implementation of IC-POVMS on Pauli channels requires prohibitive resources. The number of measurement shots required to write down an estimator,  $\hat{J}_{\mathcal{E}}$  for the Choi matrix  $J_{\mathcal{E}}$  such that any valid distance with respect to the true channel satisfies,

$$\|J_{\mathcal{E}} - \hat{J}_{\mathcal{E}}\| \leq \epsilon, \quad (23)$$

scales as  $\mathcal{O}(d^4/\epsilon^2)$ , where  $d$  is the dimension of the system's Hilbert space, and  $\epsilon \in \mathbb{R}^+$ . This scaling comes from the Choi matrix having  $\mathcal{O}(d^4)$  independent parameters (for a channel acting on a  $d$ -dimensional system). To estimate the independent parameters, the number of measurements needed typically scales inversely with the square of the desired accuracy as per the standard quantum limit [35]. Even with more modern (theoretically optimal) techniques such as Heisenberg-limited measurements [36, 37], this quartic overhead in the system dimension persists.

For channels comprising noisy qubit systems of  $N$  qubits (i.e., mixed unitary channels), this scaling makes characterising a quantum channel exponentially prohibitive, since  $d$  scales as  $\mathcal{O}(2^N)$ , hence the NP-hardness in distinguishing mixed unitary channels [17]. Here, we motivate the simple example of using the computational basis on a small number of qubits as an example of how the gauge freedoms arise when one does not measure in an informationally complete manner. This is a reasonable assumption for  $N$ -qubit Pauli channels, for which number of elements of IC POVMs scales as  $\mathcal{O}(4^N)$ . The results of this section, and for the general case of  $d$ -dimensional channels can be found in Table 1. Further discussion on the number of shots required to detect a spoofer up to some probability,  $p$ , is reserved for Sec. 6.

	$N$ qubits	qudit
Type-I Pauli	$(4^N - 2^N)/2$	—
Type-I general	$4^N - 2^N$	$d^2 - d$
Type-II Pauli	$4^N - 2^N$	—
Type-II general	$16^N - 8^N - 4^N + 2^N$	$d^4 - d^3 - d^2 + d$

Table 1: Number of free real parameters for  $N$  qubits and various types of spoofing, as well as for  $d$ -dimensional systems (qudits). Note that an  $N$ -qubit state can always be represented as a single  $2^N$ -dimensional system.

## 5.1 One Qubit

Consider the channel  $\mathcal{E} : \mathcal{B}(\mathcal{H}_2) \rightarrow \mathcal{B}(\mathcal{H}_2)$ ,

$$\mathcal{E}(\rho) = \alpha_0\rho + \alpha_1 X\rho X + \alpha_2 Y\rho Y + \alpha_3 Z\rho Z, \quad (24)$$

where the coefficients,  $\alpha_j$  sum to one,  $\rho \in \mathcal{B}_+(\mathcal{H}_2)$  is a input state, and  $\{X, Y, Z\}$  are the Pauli matrices. Using Eq. (2), the Choi matrix of the channel reads

$$J_{\mathcal{E}} = \begin{pmatrix} \alpha_0 + \alpha_3 & 0 & 0 & \alpha_0 - \alpha_3 \\ 0 & \alpha_1 + \alpha_2 & \alpha_1 - \alpha_2 & 0 \\ 0 & \alpha_1 - \alpha_2 & \alpha_1 + \alpha_2 & 0 \\ \alpha_0 - \alpha_3 & 0 & 0 & \alpha_0 + \alpha_3 \end{pmatrix}. \quad (25)$$

We may now explore our two types of spoofer on this one qubit channel.

### Type-I Spoofing

Theorem 1 forces the structure of the component  $\Phi$  of spoofing channel,  $\mathcal{E}'$ , in the natural representation to be

$$S_{\Phi} = \begin{pmatrix} 1 & 0 & 0 & 0 \\ 0 & \beta & 0 & 0 \\ 0 & 0 & \beta & 0 \\ 0 & 0 & 0 & 1 \end{pmatrix}, \quad (26)$$

such that

$$J_{\mathcal{E}'} = J_{\Phi \circ \mathcal{E}} = \begin{pmatrix} \alpha_0 + \alpha_3 & 0 & 0 & \beta(\alpha_0 - \alpha_3) \\ 0 & \alpha_1 + \alpha_1 & \beta(\alpha_1 - \alpha_2) & 0 \\ 0 & \beta(\alpha_1 - \alpha_2) & \alpha_1 + \alpha_2 & 0 \\ \beta(\alpha_0 - \alpha_3) & 0 & 0 & \alpha_0 + \alpha_3 \end{pmatrix}. \quad (27)$$

Notice that this induces the following change in the coefficients,  $\{\alpha_j\}$ , of the channel,

$$\begin{aligned} \alpha_1 - \alpha_2 &\rightarrow \beta(\alpha_1 - \alpha_2), \\ \alpha_0 - \alpha_3 &\rightarrow \beta(\alpha_0 - \alpha_3), \end{aligned} \quad (28)$$

which indicates that *a change occurs to all four coefficients* in such a way that it is not detectable by a set of compatible measurements – in this case the computational basis. Thus, the crucial question is whether the channel  $\mathcal{E}'$  preserves the diagonal of density matrices, as these are the elements where any changes would be detected by computational

basis measurements. We can show that the transformation (28) causes no such change via the natural representation, where the action on the vectorised density matrix Eq. (4) reads

$$\begin{aligned} & \begin{pmatrix} \alpha_0 + \alpha_3 & 0 & 0 & \beta(\alpha_0 - \alpha_3) \\ 0 & \alpha_1 + \alpha_1 & \beta(\alpha_1 - \alpha_2) & 0 \\ 0 & \beta(\alpha_1 - \alpha_2) & \alpha_1 + \alpha_2 & 0 \\ \beta(\alpha_0 - \alpha_3) & 0 & 0 & \alpha_0 + \alpha_3 \end{pmatrix} \begin{pmatrix} \rho_{00} \\ \rho_{01} \\ \rho_{10} \\ \rho_{11} \end{pmatrix} \\ &= \begin{pmatrix} (\alpha_0 + \alpha_3)\rho_{00} + (\alpha_1 + \alpha_2)\rho_{11} \\ \beta(\alpha_0 - \alpha_3)\rho_{01} + \beta(\alpha_1 - \alpha_2)\rho_{10} \\ \beta(\alpha_0 - \alpha_3)\rho_{10} + \beta(\alpha_1 - \alpha_2)\rho_{01} \\ (\alpha_0 + \alpha_3)\rho_{11} + (\alpha_1 + \alpha_2)\rho_{00} \end{pmatrix}. \end{aligned} \quad (29)$$

This shows explicitly how the transformations in Eq. (28) cannot change the diagonal elements (first and last) of the vectorised density matrix, despite the fact that all the coefficients of the Pauli channel do change. Thus these transformations form a gauge freedom with respect to the set of compatible measurements. Geometrically, this gauge degree of freedom corresponds to a line contained in the tetrahedron representing all valid 1-qubit Pauli channels. See Sec. 5.2 and Fig. 3 for further discussion.

### Type-II Spoofing

Next, we consider Type-II spoofing detailed in Sec. 4.2, where we find a spoofing channel which is not necessarily divisible per Fig. 2. From Theorem 4, we see that the Choi matrix is of the form

$$J_{\mathcal{E}'} = \begin{pmatrix} \alpha_0 + \alpha_3 & 0 & 0 & \gamma \\ 0 & \alpha_1 + \alpha_2 & \beta & 0 \\ 0 & \beta & \alpha_1 + \alpha_2 & 0 \\ \gamma & 0 & 0 & \alpha_0 + \alpha_3 \end{pmatrix}, \quad (30)$$

where  $\beta, \gamma \in \mathbb{R}^+$ , so that the spoofing channel is also a Pauli channel. This induces the following change in the coefficients  $\{\alpha_j\}$  of the channel,

$$\begin{aligned} \alpha_1 - \alpha_2 &\rightarrow \beta, \\ \alpha_0 - \alpha_3 &\rightarrow \gamma. \end{aligned} \quad (31)$$

Notice that this transformation leaves the sum  $\alpha_0 + \alpha_3$  and  $\alpha_1 + \alpha_2$  unchanged, and is equivalent to,

$$\begin{aligned} \alpha'_0 &= \alpha_0 + \gamma/2, \\ \alpha'_1 &= \alpha_1 + \beta/2, \\ \alpha'_2 &= \alpha_2 - \beta/2, \\ \alpha'_3 &= \alpha_3 - \gamma/2. \end{aligned} \quad (32)$$

Again, counter to the naive intuition, this spoofing channel changes *all four* of the coefficients  $\{\alpha_j\}$  despite not being detectable in the computational basis.

## 5.2 Geometric Comparison of One Qubit Channel Spoofing

To compare these two types of spoofing on one-qubit Pauli channels, observe that Type-I spoofing has a single gauge freedom,  $\{\beta\}$ , whilst Type-II spoofing has two,  $\{\beta, \gamma\}$ . The fact that there are two gauge degrees of freedom in Type-II spoofing can be visualised in the space of Pauli maps for 1 qubit, i.e., a tetrahedron,  $\mathcal{T}$ , as shown in Fig. 3.

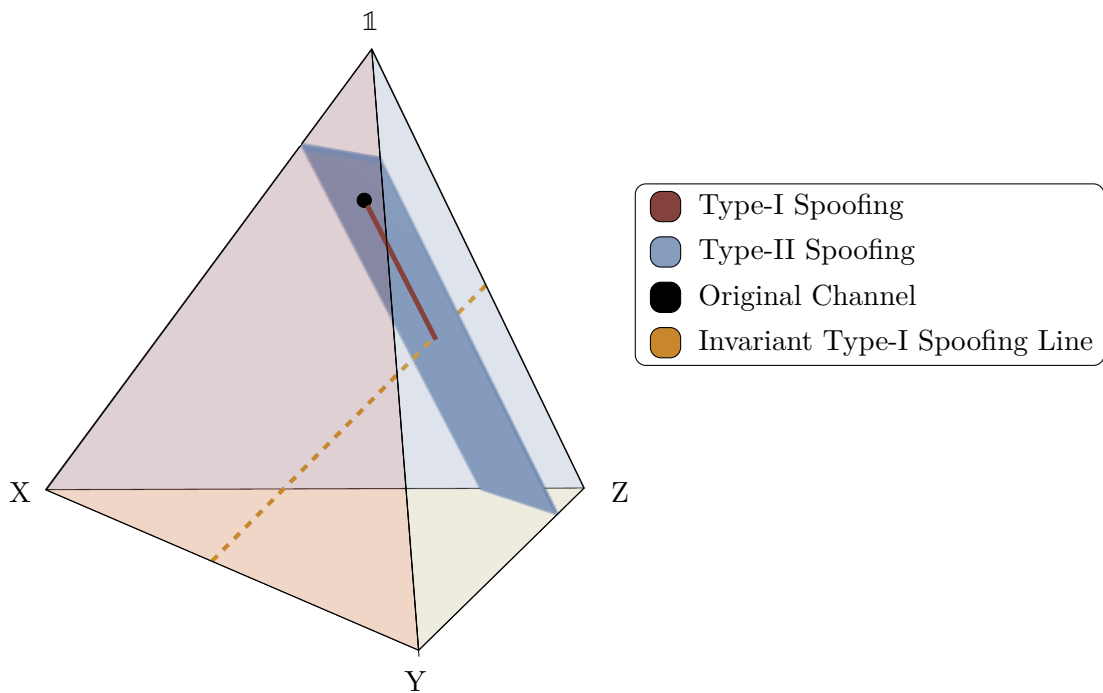


Figure 3: Comparison between Type-I and Type-II spoofers on one-qubit Pauli channels in terms of the degrees of freedom. The vertices of the tetrahedron correspond to unitary maps involving only one of the four available Pauli operators. The red (solid) line represents the single gauge degree of freedom in Type-I Spoofing, whilst the clipped blue plane represents the two degrees of freedom in Type-II Spoofing. In this form, we observe that every Type-II Spoofer is a Type-I Spoofer and not vice versa since the red dashed line is embedded in the plane. In this figure, the original Pauli channel has coefficients  $\{\alpha_0, \alpha_1, \alpha_2, \alpha_3\} = \{0.1, 0.1, 0.1, 0.7\}$ .

The two degrees of freedom means the family of Type-II spoofing channels spans a clipped-plane contained within the tetrahedron,  $\text{span}(\beta, \gamma) \cong \mathbb{R}^2 \cap \mathcal{T}$ . On the other hand, Type-I spoofing channels form a line linking the original channel to the line joining two channels,  $(\mathbb{1}\rho\mathbb{1} + Z\rho Z)/2$  and  $(X\rho X + Y\rho Y)/2$ . We can see what is so special about this line – every channel on the line is invariant under the Type-I spoofer, i.e., this family of channels does not change by varying  $\beta$ . Of note here is the fact that the Type-I line is contained within the clipped plane, meaning Type-II spoofing forms a superset of the family of spoofing channels of Type-I. In other words, *every Type-I spoofer is also a Type-II, but not every Type-II spoofer is a Type-I spoofer*. This leads us to the following corollary:

**Corollary 7.** *Type-II spoofers form a superset of Type-I spoofers, however Type-I spoofers can be applied universally with no knowledge of the original channel.*

The reason Type-I spoofing requires no prior knowledge is because it concatenates with the original channel  $\mathcal{E}$ , and its structure has no dependence on the original coefficients of the channel. We only required that the concatenation acts as the identity channel along detectable components in the natural representation. This is in contrast with Type-II spoofing, where the new Choi matrix of the spoofing channel  $J_{\mathcal{E}'}$  explicitly contains diagonal blocks whose elements take the same value as the original channel. Thus Type-II spoofing requires prior knowledge.

## 6 Discussion

In principle, quantum mechanics allows for the simultaneous measurement in any commuting basis. However, in practise, making measurements different from the computational basis is done by applying a pre-measurement local transformation [38, 39]. Provided a spoofer has knowledge of the chosen measurement basis ahead of compiling, this means spoofing any projective measurement basis is possible. This is the case in cloud-based quantum hardware, where providers know both the channel and the measurement basis before executing the channel.

Consequently, an important strategy for device certification therefore arises in this setting. Namely, one can only certify that a channel belongs to a certain spoofing equivalence class (and not certify a unique channel) due to the fact that spoofers would go undetected with projective measurements alone. Moreover, within a given equivalence class, the Kraus rank can change, which affects the simulation hardness. This in turn impacts the quantum advantage that can be certified on cloud-based quantum hardware. One way we could perform device certification in lieu of spoofing is therefore to find the *minimal* Kraus rank of a spoofing class of a given channel, see Sec. 7.1.

As briefly mentioned in the introduction, one might argue that techniques like classical shadows [25] (introducing classical randomness into measurements) mean that we can perform informationally complete measurements. In this sense, an inherent amount of classical randomness could protect against spoofing. This is allowed by an adversary when we consider that adding classical randomness is within the bounds of mixed unitary channels in the first place. However, even with classical randomness, we would only be able to detect a spoofer when given access to exponential resources. This is because we need to estimate the full quantum channel to detect a spoofer, requiring a large dataset which is exponential in the number of bodies – hence why distinguishing quantum channels is a QIP-hard problem [24]. This is irrespective of the fact that it is possible to make an outcome distribution which is *technically* informationally complete.

For a small system, our spoofer would therefore easily be detected. But with the promise of quantum devices to scale to many hundreds of qubits, acquiring sufficient amounts of data to fully characterise a quantum channel is prohibitively expensive. This is what we may exploit in order to design spoofing strategies. A spoofer can go undetected when the dataset used to characterise a channel is sub-exponential in the number of shots. However, the spoofer will only go undetected with some success probability, as the randomness of the shadow-based measurements means that certain changes could be identified. For example, a user who wishes to certify a channel on  $N$ -qubit system with  $M$  shots will detect the spoofer with probability  $p \sim \mathcal{O}(M/4^N \epsilon^2)$ , for a precision  $\epsilon$ , as highlighted in Sec. 5.

One might argue that a valid defense strategy against this scenario is to attempt to characterise a quantum channel’s Choi matrix to an accuracy of  $\epsilon$ . Whilst this requires exponential resources in general, much attention has been given to trying to lower this complexity overhead. For example, recent works such as [40] have used a tensor network representation of the Choi matrix estimator  $\hat{J}_{\mathcal{E}}$ , meaning that their search space forms a polynomially-scaling sub-manifold of the space of channels. However, tensor networks suffer from the so-called entanglement area law [41], meaning they cannot be used to certify channels with higher entropy than permitted by this approximation. From an adversarial perspective, this leaves a spoofer with the option to vary elements of a Choi matrix that are not captured by this representation. In other words, by changing the channel such that its reduction under these changes to a tensor network representation is undetectable, an adversary can still cause a user to falsely certify a quantum channel’s Choi matrix.

## 6.1 Spoofer with Minimal Kraus Rank

In the above, we alluded to the complications that arise when attempting to certify a quantum channel in cloud-based settings due to the fact that spoofing equivalence classes contain channels with differing Kraus rank. In this subsection, we highlight the importance of being able to determine the *minimum* Kraus rank of a given equivalence class for quantum advantage, quantum simulation, and variational quantum channels.

Consider the scenario where a user wishes to certify the quantum advantage of a device being managed by an untrusted adversary, for example in cloud-based quantum hardware. In order to certify that their device provides quantum advantage, they may choose to estimate the simulation hardness of the device's quantum channel representation, using a measure such as the Kraus rank (i.e., the number of non-zero eigenvalues of the channel's Choi matrix). In the case where a user has access only to projective measurements in a specified basis, the adversary providing the channel is free to vary the other parameters of the Choi matrix that define its equivalence class. Therefore a user must know the minimal Kraus rank of their quantum process, or risk being misled about its resource requirements. This is because members of the spoofer's equivalence class can range from  $d$  to  $d^2$  for a  $d$ -dimensional quantum channel. Since the adversarial hardware provider will know both the channel *and* measurements before compiling, it is possible for the adversary to simulate a user's quantum process in such a way that the actual channel being run on the device has a lower Kraus rank than the one a user intended. Furthermore, since these changes leave the marginals of the user's measurements unchanged, any changes made by the adversarial provider are undetectable by the user. It is therefore of critical importance for users to be able to find the channel realizing minimum Kraus rank inside a given equivalence class in order to defend against this adversarial strategy.

Within a spoofing equivalence class, we can also consider the significance of a channel with minimal Kraus rank in variational settings. The minimal Kraus rank of a variational channel's spoofer could be considered as a way of establishing the extent to which an equivalence class is subject to the trade-off between barren plateaus and expressiveness when solving variational problems. Under our current measurement scheme, the minimum Kraus rank is fixed for all  $d$ -dimensional quantum channels. However, this minimum rank may change for different measurement schemes, (see Sec. 8 for further discussion on various measurement classes). Our contribution shows how a measurement scheme induces an equivalence class for channels in terms of their outcome distributions. The minimal Kraus rank of these classes could be considered as the open system equivalent of the work of Ref. [42]. In this paper, the authors show how to quantify barren plateaus by considering the dynamical Lie algebra that generates dynamics and measurements on unitary settings. Using our contribution, we can think of the minimum Kraus rank of our equivalence class as the open system analogue, as this rank is irreducible. This would allow us to establish and quantify barren plateau phenomena for variational channels like those of Ref. [27]. Evidently, our analogy behind these gauges and their significance to quantum channels is only an intuition, since quantum channels form a semi-group, rather than a group [8].

## 7 Finding Spoofer with Minimal Kraus Rank

Having found the structure of the spoofing families in Section 4, we are in a position to solve the practical problem of minimising the Kraus rank of a given channel  $\mathcal{E}$  (for the discussion of its importance, see Sec. 6). Specifically, we seek a channel  $\mathcal{E}'$  belonging to the Type-II spoofing family of the original channel  $\mathcal{E} \sim_{\mathcal{M}} \mathcal{E}'$ , such that the Kraus rank of

$\mathcal{E}'$  is the smallest of its equivalence class defined by Eq. (7). There are two algorithms that can numerically tackle this problem, both reducing the Kraus rank from a generic  $d^2$  to  $d$  for a  $d$ -dimensional quantum channel. One is based on the Sinkhorn algorithm [43] and relies on singular value decomposition, whilst the other is based on conic programming and Linear Matrix Inequalities (LMIs). Whilst the latter offers a nice geometric intuition, it is recursive, meaning it is inefficient for large system sizes. As such, a discussion of the LMI-based rank reduction is reserved for App. D. Here, we instead focus on the Sinkhorn-like algorithm [43] for lowering the Kraus rank of a channel in Sec 7.1. We also provide an analytic algorithm to minimize their Kraus rank to its minimum bound for the special case of Pauli channels in Sec 7.2.

For a generic channel, we note that no further lowering is possible, as the rank of the Choi matrix cannot be smaller than the rank of its sub-matrices. Therefore, it suffices that at least one of  $d \times d$  diagonal blocks of the Choi matrix of the channel is of full rank to restrict the lowest possible Kraus rank of any channel in its spoofing equivalence class to  $d$ . Given that both our algorithms achieve this value, we conclude that they fully solve the rank problem for spoofing of channels. A `Mathematica` implementation of the Sinkhorn-like algorithm can be found at GitHub [44].

### 7.1 Sinkhorn-like Algorithm for an Arbitrary Channel

This numerical algorithm uses an analogous reasoning to the Sinkhorn algorithm [43], which was first used to generate bistochastic matrices. We start with a  $d$ -dimensional quantum channel,  $\mathcal{E}$ , generically of Kraus rank  $d^2$ . Our aim is to find a channel in the same spoofing equivalence class which achieves the minimal Kraus rank  $d$ . We start out by finding the closest matrix via a low-rank approximation [45, 46]. However, in general this closest matrix will not be a valid Choi matrix. Therefore, to properly lower the rank we need to take into account two factors: (i) the usual conditions for the Choi matrix to be a CPTP map, and (ii) we must ensure that diagonal blocks of its Choi matrix are equal to the ones of the original channel, per Theorem. 4.

To simultaneously satisfy these two factors, we may alternate between them, as shown in Algorithm 1. In the algorithm, by  $\{\lambda_i\}_{i=1}^{d^2}$  we refer to the eigenvalues of the current Choi matrix in decreasing order, while  $[J_{\mathcal{E}'}]_{ij}$  denotes the  $\{i, j\}$ -th block of dimension  $d \times d$  of the matrix  $J_{\mathcal{E}'}$ .



---

**Algorithm 1** Sinkhorn-like lowering the Kraus rank of a channel
 

---

- 1: **Input:** Choi matrix,  $J_{\mathcal{E}}$ , of the original channel  $\mathcal{E}$  of rank up to  $d^2$ .
  - 2:  $J_{\mathcal{E}'} \leftarrow J_{\mathcal{E}}$
  - 3: **while**  $\lambda_{d+1} > \epsilon$  **do**
  - 4:    $J_{\mathcal{E}'} = UDU^\dagger$   $\triangleright$  Find the low-rank approximation to Choi matrix  $J_{\mathcal{E}'}$  via singular value decomposition
  - 5:    $J_{\mathcal{E}'} \leftarrow U_d D_d U_d^\dagger$   $\triangleright$  Truncate the matrices by discarding all but  $d$  largest singular values
  - 6:   Set the diagonal blocks of  $J_{\mathcal{E}'}$  to be equal to the original  $J_{\mathcal{E}}$
  - 7:   **for**  $i \in \{1, \dots, d\}$  **do**
  - 8:      $[J_{\mathcal{E}'}]_i \leftarrow [J_{\mathcal{E}}]_i$
  - 9:   **end for**
  - 10:   **for**  $i, j \in \{1, \dots, d\}, i \neq j$  **do**
  - 11:      $[J_{\mathcal{E}'}]_{ij} \leftarrow [J_{\mathcal{E}'}]_{ij} - \mathbb{1} \text{Tr}([J_{\mathcal{E}'}]_{ij})/d$   $\triangleright$  Set the off-diagonal blocks to be traceless
  - 12:   **end for**
  - 13:    $J_{\mathcal{E}'} \leftarrow \frac{1}{2}(J_{\mathcal{E}'} + J_{\mathcal{E}'}^\dagger)$   $\triangleright$  Make the Choi matrix Hermitian
  - 14: **end while**
  - 15: **Output:** Choi matrix  $J_{\mathcal{E}'}$  of rank  $d$  in the same equivalence class as  $\mathcal{E}$  defined by Eq. (7).
- 

The algorithm produces the spoofing channel,  $\mathcal{E}'$ , with minimal Kraus rank  $d$ , in its Type-II spoofing equivalence class, in which the original channel,  $\mathcal{E}$ , is also a member. That is, by using  $\mathcal{E}'$ , we reduce the Kraus rank from  $d^2$  (in the generic case) to  $d$  whilst maintaining the exact marginals for a projective measurement, per Eq. (7). All of the initial channels,  $\mathcal{E}$ , that we have tested through Algorithm 1 have produced a channel of the minimal rank in their equivalence class, suggesting that the algorithm may work generally for any input channel. Importantly, the convergence rate of the eigenvalues is exponential, as shown in Fig. 4 for an exemplary channel of dimension 20. We observed the complexity growth that scales with the dimension of the system as  $d^4$ , reflecting the growing number of parameters that describe a channel.

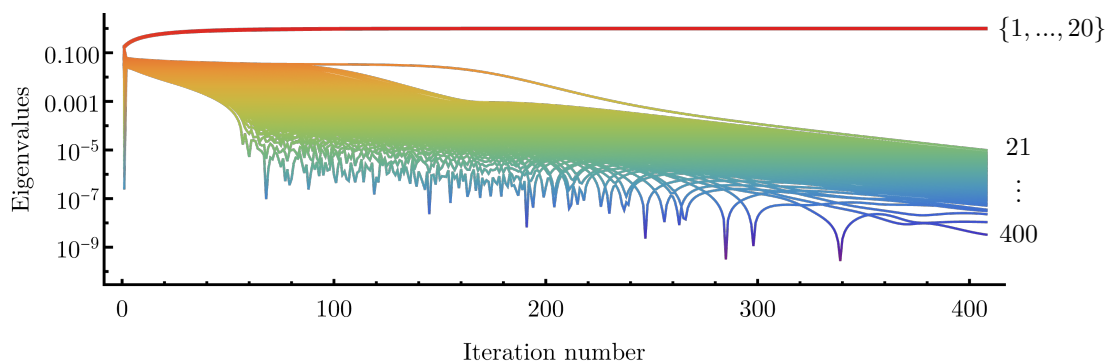


Figure 4: The convergence of eigenvalues of the Choi matrix of a generic  $d = 20$  dimensional quantum channel under Sinkhorn-like algorithm [43]. Out of  $20^2 = 400$  eigenvalues, 20 are positive, denoted by  $\{1, \dots, 20\}$  in the figure, while the rest exponentially converge to zero. By setting a tolerance value, we can therefore set these exponentially vanishing eigenvalues to zero, finding the Type-II spoofing matrix for the projective measurement set defined in Sec. 3.

## 7.2 Analytical Spoofing Algorithm for Pauli Channels

The algorithm detailed above may be universal in the sense that it works for any arbitrary channel in  $d$ -dimensions. However, it runs numerically, which can be cumbersome as the system size grows. Here, we propose an algorithm for lowering the rank that is specifically tailored to Pauli channels, with the added advantage of being analytical. It shows that any  $N$ -qubit Pauli channel's projective marginals can be simulated by a quantum channel with Kraus rank  $d$ .

Let us start with a simple observation concerning Choi matrix of a Pauli channel on  $N$  qubits, defined by its Kraus operators  $\{\sqrt{\alpha_i}P_i\}_i$ . The location of non-zero elements for each of the  $4^N$  rows in the Choi matrix forms a pattern which is repeated  $2^N$  times. To see how this works, we consider the example shown Fig. 5 for 2- and 3-qubit channels, which shows that the same pattern of non-zero elements repeats itself four and eight times respectively for 2- and 3-qubit channels.

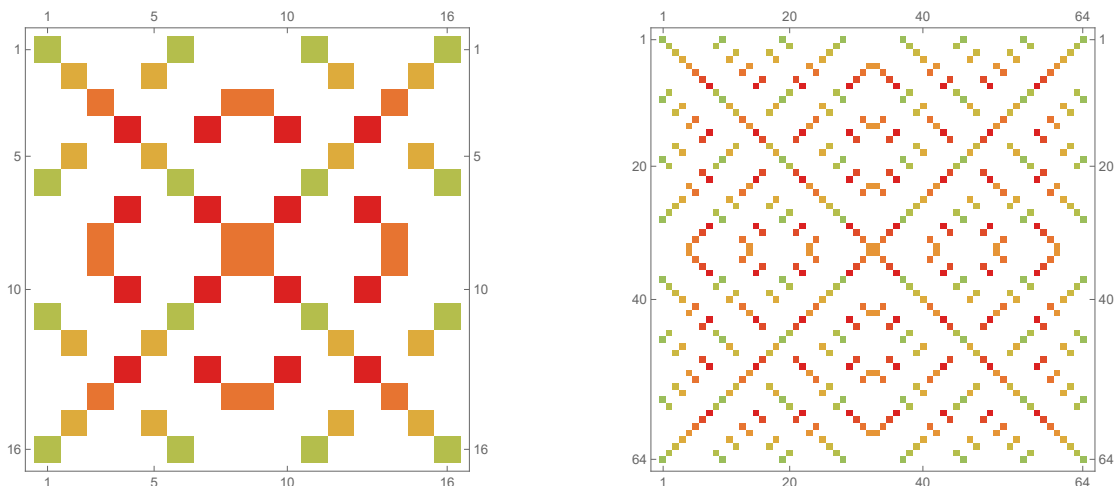


Figure 5: The non-zero patterns for 2-qubit (left panel) and 3-qubit (right panel) Choi matrices for Pauli channels, where the colors distinguish between different patterns. Observe that, for example, in the left panel rows: 1, 6, 11, and 16 share the same pattern of non-zero elements. In total, there are  $2^N = 4$  and 8 different patterns respectively for 2-qubit and 3-qubit channels.

A given Kraus coefficient of the Pauli channel,  $\sqrt{\alpha_i}$ , corresponds to a unique non-zero pattern which is repeating. For each of the sets, we may take the full set of the corresponding coefficients  $\{\alpha_i\}_{i \in S}$  and sum them, obtaining  $\beta_S = \sum_{i \in S} \alpha_i$ . Then, by setting one of these coefficients to be equal to  $\beta_S$  and the rest to 0, we do not leave the Type-II spoofing equivalence class of the original channel. Consequently, the Kraus rank of the channel lowers quadratically, from generic  $4^N$  to  $2^N$ . This result is analogous to Algorithm 1 from the previous subsection, but works analytically. The advantage of this algorithm comes from engineering linear dependence via an analytical change of the free parameters.

As an example, consider the action of this algorithm on an arbitrary 1-qubit Pauli channel  $J_{\mathcal{E}} \mapsto J_{\mathcal{E}'}$  as

$$J_{\mathcal{E}} = \begin{pmatrix} \alpha_0 + \alpha_3 & 0 & 0 & \alpha_0 - \alpha_3 \\ 0 & \alpha_1 + \alpha_2 & \alpha_1 - \alpha_2 & 0 \\ 0 & \alpha_1 - \alpha_2 & \alpha_1 + \alpha_2 & 0 \\ \alpha_0 - \alpha_3 & 0 & 0 & \alpha_0 + \alpha_3 \end{pmatrix} \mapsto J_{\mathcal{E}'} = \begin{pmatrix} \alpha'_0 & 0 & 0 & \alpha'_0 \\ 0 & \alpha'_1 & \alpha'_1 & 0 \\ 0 & \alpha'_1 & \alpha'_1 & 0 \\ \alpha'_0 & 0 & 0 & \alpha'_0 \end{pmatrix}, \quad (33)$$

where  $\alpha'_0 = \alpha_0 + \alpha_3$  and  $\alpha'_1 = \alpha_1 + \alpha_2$ . We see that the new channel  $\mathcal{E}'$  is in the same equivalence class as  $\mathcal{E}$ , but with Kraus rank equal to 2 instead of 4. For further explanation of this algorithm we refer the reader to our Github code [44].

## 8 Concluding Remarks

One of the most important problems in characterising quantum devices is determining the quantum channel representation of their evolution. In this contribution, we have first illustrated a key consequence of the QIP-hardness of quantum channel discrimination [24]. Namely, one cannot establish a direct link (i.e., with full certainty) between outcome statistics and Choi matrices for quantum channels with sub-exponential resources. We have laid grounds, based on this complexity, for spoofing an arbitrary quantum channel in  $d$ -dimensional Hilbert space in such a way that its Kraus rank can be lowered from generic  $d^2$  to  $d$ . This can be done in an undetectable way for fixed measurement bases, while the success probability of detection under shadow-based measurements scales as  $\mathcal{O}(M/d^2)$ . Given the Choi matrix,  $J_{\mathcal{E}}$ , of any quantum channel,  $\mathcal{E}$ , we showed how to find this minimum via a Sinkhorn-like algorithm, whose efficacy was numerically demonstrated for quantum channels up to dimension 20. For the case of Pauli channels, the same improvement for the minimal Kraus rank was found analytically in a single step by engineering linear dependence of rows in the Choi representation. Our findings open new avenues for efficient quantum channel simulation and adversarial spoofing strategies. They also improve the understanding of the extent to which variational quantum channels might be subject to the trade-off between barren plateaus and expressiveness.

Given our findings, one might wonder how the number of gauge degrees of freedom changes when we allow for more than one projective measurement. Specifically, we can refine the equivalence classes by appending more bases to the permitted measurement set  $\mathcal{M}$  from Eq. (6). For example, if we allow

$$\mathcal{M} = \{|q\rangle\langle q|, U_1 |q\rangle\langle q| U_1^\dagger, U_2 |q\rangle\langle q| U_2^\dagger, \dots, U_{k-1} |q\rangle\langle q| U_{k-1}^\dagger\}, \quad (34)$$

we could establish a minimal Kraus rank which goes from  $d^2 \rightarrow f(k)d$  under this larger set of projective measurements, for some  $f(k)$  to be determined. Another future direction is to determine how an equivalence class may be structured when we instead require that the spoofing channel has the same outcome statistics up to a given polynomial order in the moments of outcome distributions. This would re-frame the spoofing families' equivalence classes to be effective for any projective measurement for finite statistics. We leave these suggestions as open problems for the quantum information community.

## Acknowledgements

We would like to thank Jakub Czartowski, Jarosław Korbicz, Marcin Płodzień, José Ramón Martínez, Antonio Acín, and Karol Życzkowski for fruitful discussions and comments.

This project was supported by Government of Spain (Severo Ochoa CEX2019-000910-S, Quantum in Spain, FUNQIP and European Union NextGenerationEU PRTR-C17.I1), the European Union (PASQuanS2.1, 101113690 and Quanteria Veriqtas), Fundació Cellex, Fundació Mir-Puig, Generalitat de Catalunya (CERCA program), the ERC AdG CERQUTE and the AXA Chair in Quantum Information Science.

## References

- [1] D. Gottesman. *Stabilizer codes and quantum error correction*. California Institute of Technology, 1997.
- [2] J. Preskill. “Reliable quantum computers”. In: *Proc. of the Royal Soc. A* 454 (1998), pp. 385–410.
- [3] R. Raussendorf. “Key ideas in quantum error correction”. In: *Philos. Trans. R. Soc. A* 370 (2012), pp. 4541–4565.
- [4] B. A. Bell et al. “Experimental demonstration of a graph state quantum error-correction code”. In: *Nature Communications* 5 (2014), p. 3658.
- [5] Z. Cai et al. “Quantum error mitigation”. In: *Reviews of Modern Physics* 95 (2023), p. 045005.
- [6] S. Endo, S. C. Benjamin, and Y. Li. “Practical quantum error mitigation for near-future applications”. In: *Physical Review X* 8 (2018), p. 031027.
- [7] K. Temme, S. Bravyi, and J. M. Gambetta. “Error mitigation for short-depth quantum circuits”. In: *Physical Review Letters* 119 (2017), p. 180509.
- [8] H.-P. Breuer and F. Petruccione. *The theory of open quantum systems*. Oxford University Press, USA, 2002.
- [9] B. M. Terhal et al. “Simulating quantum operations with mixed environments”. In: *Phys. Rev. A* 60 (1999), p. 881. DOI: [10.1103/PhysRevA.60.881](https://doi.org/10.1103/PhysRevA.60.881).
- [10] G. Narang and Arvind. “Simulating a single-qubit channel using a mixed-state environment”. In: *Phys. Rev. A* 75 (2007), p. 032305. DOI: [10.1103/PhysRevA.75.032305](https://doi.org/10.1103/PhysRevA.75.032305). URL: <https://link.aps.org/doi/10.1103/PhysRevA.75.032305> (visited on 01/25/2019).
- [11] E. Jung et al. “Amplitude damping for single-qubit system with single-qubit mixed-state environment”. In: *J. Phys. A: Math. Theor.* 41 (2008), p. 045306. ISSN: 1751-8121. DOI: [10.1088/1751-8113/41/4/045306](https://doi.org/10.1088/1751-8113/41/4/045306). URL: <https://doi.org/10.1088/1751-8113/41/4/045306>.
- [12] A. Müller-Hermes and C. Perry. “All unital qubit channels are 4-noisy operations”. In: *Lett. Math. Phys.* 109 (2019), p. 1. DOI: [10.1007/s11005-018-1104-x](https://doi.org/10.1007/s11005-018-1104-x). URL: <https://doi.org/10.1007/s11005-018-1104-x>.
- [13] C. Zheng. “Universal quantum simulation of single-qubit nonunitary operators using duality quantum algorithm”. In: *Sci. Rep.* 11 (2021), p. 3960.
- [14] M. E. Shirokov. “Strong convergence of quantum channels: Continuity of the Stinespring dilation and discontinuity of the unitary dilation”. In: *J. Math. Phys.* 61 (2020), p. 082204.
- [15] A. Gaikwad, Arvind, and K. Dorai. “Simulating open quantum dynamics on an NMR quantum processor using the Sz.-Nagy dilation algorithm”. In: *Phys. Rev. A* 106 (2022), p. 022424.
- [16] K. Wang and D. Wang. “Quantum circuit simulation of superchannels”. In: *New Journal of Physics* 25 (2023), p. 043013. ISSN: 1367-2630. DOI: [10.1088/1367-2630/acc5aa](https://doi.org/10.1088/1367-2630/acc5aa). URL: <http://dx.doi.org/10.1088/1367-2630/acc5aa>.
- [17] C. Lee and J. Watrous. “Detecting mixed-unitary quantum channels is NP-hard”. In: *Quantum* 4 (2020), p. 253. ISSN: 2521-327X. DOI: [10.22331/q-2020-04-16-253](https://doi.org/10.22331/q-2020-04-16-253). URL: <http://dx.doi.org/10.22331/q-2020-04-16-253>.

- [18] M. Girard and J. Levick. “Twirling channels have minimal mixed-unitary rank”. In: *Linear Algebra and its Applications* 615 (2021), pp. 207–227. ISSN: 0024-3795. DOI: 10.1016/j.laa.2020.12.027. URL: <http://dx.doi.org/10.1016/j.laa.2020.12.027>.
- [19] M. Girard et al. “On the Mixed-Unitary Rank of Quantum Channels”. In: *Communications in Mathematical Physics* 394 (2022), pp. 919–951. ISSN: 1432-0916. DOI: 10.1007/s00220-022-04412-y. URL: <http://dx.doi.org/10.1007/s00220-022-04412-y>.
- [20] C. Lancien and A. Winter. “Approximating quantum channels by completely positive maps with small Kraus rank”. In: *Quantum* 8 (2024), p. 1320. ISSN: 2521-327X. DOI: 10.22331/q-2024-04-30-1320. URL: <https://doi.org/10.22331/q-2024-04-30-1320>.
- [21] J. Peetz et al. “Simulation of open quantum systems via low-depth convex unitary evolutions”. In: *Physical Review Research* 6 (2024). ISSN: 2643-1564. DOI: 10.1103/physrevresearch.6.023263. URL: <http://dx.doi.org/10.1103/PhysRevResearch.6.023263>.
- [22] I. Bengtsson and K. Życzkowski. *Geometry of quantum states: an introduction to quantum entanglement*. Cambridge University Press, 2017.
- [23] S. Flammia and J. Wallman. “Efficient Estimation of Pauli Channels”. In: *ACM Transactions on Quantum Computing* 1 (2020), pp. 1–32. ISSN: 2643-6817. DOI: 10.1145/3408039. URL: <http://dx.doi.org/10.1145/3408039>.
- [24] B. Rosgen. “Computational distinguishability of quantum channels”. In: *arXiv preprint arXiv:0909.3930* (2009).
- [25] H. Huang, R. Kueng, and J. Preskill. “Predicting many properties of a quantum system from very few measurements”. In: *Nature Physics* 16 (2020), pp. 1050–1057. ISSN: 1745-2481. DOI: 10.1038/s41567-020-0932-7. URL: <http://dx.doi.org/10.1038/s41567-020-0932-7>.
- [26] R. Levy, D. Luo, and B. Clark. “Classical shadows for quantum process tomography on near-term quantum computers”. In: *Physical Review Research* 6 (2024). ISSN: 2643-1564. DOI: 10.1103/physrevresearch.6.013029. URL: <http://dx.doi.org/10.1103/PhysRevResearch.6.013029>.
- [27] L. Gravina and V. Savona. “Adaptive variational low-rank dynamics for open quantum systems”. In: *Physical Review Research* 6 (2024), p. 023072.
- [28] M. Ioannou et al. “Simulability of high-dimensional quantum measurements”. In: *Physical Review Letters* 129 (2022), p. 190401.
- [29] B. Zhao, K. Ito, and K. Fujii. *Probabilistic channel simulation using coherence*. 2024. DOI: 10.48550/ARXIV.2404.06775. URL: <https://arxiv.org/abs/2404.06775>.
- [30] C. Burdine et al. *Efficient Simulation of Open Quantum Systems on NISQ Devices*. 2024. DOI: 10.48550/ARXIV.2410.10732. URL: <https://arxiv.org/abs/2410.10732>.
- [31] C. Wadhwa et al. *Agnostic Process Tomography*. 2024. DOI: 10.48550/ARXIV.2410.11957. URL: <https://arxiv.org/abs/2410.11957>.
- [32] J. Watrous. *The theory of quantum information*. Cambridge University Press, 2018.
- [33] M. M. Wolf and J. I. Cirac. “Dividing Quantum Channels”. In: *Commun. Math. Phys.* 279 (2008), 147–168.

- [34] D. Davalos and M. Ziman. “Quantum dynamics is not strictly bidivisible”. In: *Physical Review Letters* 130 (2023), p. 080801.
- [35] V. B. Braginsky and F. Y. Khalili. *Quantum measurement*. Cambridge University Press, 1995.
- [36] M. Zwiernik, C. A. Pérez-Delgado, and P. Kok. “Ultimate limits to quantum metrology and the meaning of the Heisenberg limit”. In: *Physical Review A* 85 (2012), p. 042112.
- [37] R. Demkowicz-Dobrzański, J. Kołodyński, and M. Guţă. “The elusive Heisenberg limit in quantum-enhanced metrology”. In: *Nature Communications* 3 (2012), p. 1063.
- [38] H.-Y. Huang, R. Kueng, and J. Preskill. “Predicting many properties of a quantum system from very few measurements”. In: *Nature Physics* 16 (2020), pp. 1050–1057.
- [39] G. García-Pérez et al. “Learning to measure: Adaptive informationally complete generalized measurements for quantum algorithms”. In: *PRX Quantum* 2 (2021), p. 040342.
- [40] G. Torlai et al. “Quantum process tomography with unsupervised learning and tensor networks”. In: *Nature Communications* 14 (2023), p. 2858.
- [41] P. Calabrese and J. Cardy. “Entanglement entropy and quantum field theory”. In: *Journal of Statistical Mechanics: Theory and Experiment* 2004 (2004), P06002.
- [42] M. Ragone et al. “A unified theory of barren plateaus for deep parametrized quantum circuits”. In: *arXiv preprint arXiv:2309.09342* (2023).
- [43] R. Sinkhorn and P. Knopp. “Concerning nonnegative matrices and doubly stochastic matrices”. In: *Pacific Journal of Mathematics* 21 (1967), pp. 343–348.
- [44] *Low-rank simulation of quantum channels*. 2024. URL: <https://github.com/TimothyHeightman/LowRankQuantumChannels>.
- [45] E. Schmidt. “Zur Theorie der linearen und nichtlinearen Integralgleichungen: I. Teil: Entwicklung willkürlicher Funktionen nach Systemen vorgeschriebener”. In: *Mathematische Annalen* 63 (1907), pp. 433–476. ISSN: 1432-1807. DOI: [10.1007/bf01449770](https://doi.org/10.1007/bf01449770). URL: <http://dx.doi.org/10.1007/BF01449770>.
- [46] C. Eckart and G. Young. “The approximation of one matrix by another of lower rank”. In: *Psychometrika* 1 (1936), pp. 211–218. ISSN: 1860-0980. DOI: [10.1007/bf02288367](https://doi.org/10.1007/bf02288367). URL: <http://dx.doi.org/10.1007/BF02288367>.

## A Matrix Reshuffling

We can switch to the Choi representation from the natural representation via a reshuffling operation,  $S_{\mathcal{E}} \xrightarrow{R} J_{\mathcal{E}}$ . The simplest way to understand reshuffling is through double indices

$$M_{ij,kl}^R = M_{ik,jl}. \quad (35)$$

In terms of the matrix-form of Eq. (4), this reshuffling is enacted by

$$\begin{aligned} S_{ijkl} &\mapsto J_{\mu\nu} \text{ s.t.} \\ (i, j) &\mapsto \mu = d(i-1) + k, \\ (k, l) &\mapsto \nu = d(j-1) + l. \end{aligned} \quad (36)$$

## B Conditions to Simulate a Channel in Kraus Representation

To simultaneously satisfy Eq. (6) and Eq. (9), we require two types of conditions for the Kraus operators,:

- **Condition 1** – for all input states and measurement outcomes,

$$\sum_{r=0}^R \sum_{m,n=0}^{d-1} K_{qn}^{(r)} \rho_{nm} K_{mq}^{(r)\dagger} = \sum_{r=0}^R \sum_{m,n=0}^{d-1} K_{qn}^{l(r)} \rho_{nm} K_{mq}^{l(r)\dagger}, \quad (37)$$

where  $K_{qn}^{(r)}$  (resp.  $K_{qn}^{l(r)}$ ) form a Kraus representation of the channel  $\mathcal{E}$  (resp.  $\mathcal{E}'$ ).

- **Condition 2** – there exist values for the indices  $\{i, j, k, l\} \in \{0, \dots, d-1\}$  such that

$$\sum_{r=0}^R \sum_{l,n=0}^{d-1} \left( K_{ki}^{(r)} K_{nj}^{(r)\dagger} - K_{ki}^{l(r)} K_{nj}^{l(r)\dagger} \right) \neq 0. \quad (38)$$

Eq. (37) is simply a restatement of Eq. (6) at the level of Kraus operators. To see why this is the case, consider calculating the outcome probability

$$p_{\mathcal{E}}(q|\rho) = \text{Tr}(\mathcal{E}(\rho) |q\rangle\langle q|). \quad (39)$$

As introduced above, let the POVM set be computational basis measurements. In this basis, the Kraus operators of  $\mathcal{E}$  are,

$$K^{(r)} = \sum_{i,j=0}^{d-1} K_{i,j}^{(r)} |i\rangle\langle j|, \quad (40)$$

whilst the state,  $\rho = \sum_{n,m} \rho_{nm} |n\rangle\langle m|$ . In this basis, we can express the action of  $\mathcal{E}$  as,

$$\begin{aligned} \mathcal{E}(\rho) &= \sum_{r=0}^R \sum_{i,j,k,l,m,n=0}^{d-1} K_{ij}^{(r)} |i\rangle\langle j| \rho_{nm} |n\rangle\langle m| K_{kl}^{(r)\dagger} |l\rangle\langle k|. \\ &= \sum_{r=0}^R \sum_{i,l,m,n=0}^{d-1} K_{in}^{(r)} \rho_{nm} K_{ml}^{(r)\dagger} |i\rangle\langle l|. \end{aligned} \quad (41)$$

This allows us to calculate the outcome probabilities

$$\begin{aligned} \text{Tr}(\mathcal{E}(\rho) |q\rangle\langle q|) &= \text{Tr} \left( \sum_{r=0}^R \sum_{i,l,m,n=0}^{d-1} K_{in}^{(r)} \rho_{nm} K_{ml}^{(r)\dagger} |i\rangle\langle l| |q\rangle\langle q| |l\rangle\langle q| \right) \\ &= \sum_{r=0}^R \sum_{i,l,m,n=0}^{d-1} K_{in}^{(r)} \rho_{nm} K_{ml}^{(r)\dagger} \text{Tr}(|i\rangle\langle l| |q\rangle\langle q| |l\rangle\langle q|) \\ &= \sum_{r=0}^R \sum_{m,n=0}^{d-1} K_{qn}^{(r)} \rho_{nm} K_{mq}^{(r)\dagger}. \end{aligned} \quad (42)$$

Let us understand this form a little better. First, this condition is over the *sum* of Kraus operators. Thus, each Kraus matrix (or any subset thereof) can be different provided the *collective* action on the state  $\rho$  is the same. Second, both the left-hand side and the right-hand side have  $R + 1$  Kraus operators, but in general this is not necessary since they are

both summer over. This shows why a spoofing channel can in principle have a lower rank than the original channel, provided each term in the sum contributes on average a larger amount to this probability.

We can summarise this by requiring

$$\sum_{r=0}^R \sum_{m,n=0}^{d-1} K_{qn}^{(r)} \rho_{nm} K_{mq}^{(r)\dagger} = \sum_{r=0}^{R'} \sum_{m,n=0}^{d-1} K_{qn}^{(r')} \rho_{nm} K_{mq}^{(r')\dagger}, \quad R' \leq R, \quad \forall q \in \{0, d-1\}, \quad (43)$$

which takes into account the above points. Hence, we see that demanding the outcome probabilities be the same irrespective of the input state is simply requiring Eq. (37) at the level of Kraus operators.

The second condition we require is that the Choi matrices be different. Eq. (38) is simply a statement of this at the level of Kraus operators. Recall that the Choi matrix of a channel  $\mathcal{E}$  can be expressed in the computational basis via Kraus operators,

$$\begin{aligned} J_{\mathcal{E}} &= (\mathbb{1} \otimes \mathcal{E}) \sum_{ij=0}^{d-1} |i\rangle\langle j| \otimes |i\rangle\langle j| \\ &= \sum_{kij=0}^{d-1} |k\rangle\langle k|i|k|i\rangle \langle j| \otimes \mathcal{E}(|i\rangle\langle j|) \\ &= \sum_{ij=0}^{d-1} \left( |i\rangle\langle j| \otimes \sum_{r=0}^R \sum_{klmn=0}^{d-1} K_{kl}^{(r)} |k\rangle\langle l|i|l|i\rangle \langle j|m|j|m\rangle \langle n| K_{nm}^{(r)\dagger} \right) \\ &= \sum_{ij=0}^{d-1} \left( |i\rangle\langle j| \otimes \sum_{r=0}^R \sum_{ln=0}^{d-1} K_{ki}^{(r)} K_{nj}^{(r)\dagger} |k\rangle\langle n| \right) \\ &= \sum_{r=0}^R \sum_{ijln=0}^{d-1} |i\rangle\langle j| \otimes K_{ki}^{(r)} K_{nj}^{(r)\dagger} |k\rangle\langle n|. \end{aligned} \quad (44)$$

Hence, the requirement that the two Choi matrices,  $J_{\mathcal{E}}$  and  $J_{\mathcal{E}'}$ , be different can be expressed as requiring the *difference* between the two to be non-zero. Assuming the same Kraus rank for both channels, we require

$$\sum_{r=0}^R \sum_{ijln=0}^{d-1} |i\rangle\langle j| \otimes K_{ki}^{(r)} K_{nj}^{(r)\dagger} |k\rangle\langle n| - \sum_{r=0}^R \sum_{ijln=0}^{d-1} |i\rangle\langle j| \otimes K_{ki}^{(r')} K_{nj}^{(r')\dagger} |k\rangle\langle n| \neq \mathbb{0}, \quad (45)$$

where  $\mathbb{0}$  is the matrix of 0s in dimension  $d^2$ . By factorising the left hand side of the tensor product, this expression can be simplified to

$$\sum_{ij=0}^{d-1} |i\rangle\langle j| \otimes \sum_{r=0}^R \sum_{ln=0}^{d-1} \left( K_{ki}^{(r)} K_{nj}^{(r)\dagger} - K_{ki}^{(r')} K_{nj}^{(r')\dagger} \right) |k\rangle\langle n| \neq \mathbb{0}. \quad (46)$$

Since the LHS of the tensor product has coefficients 1 for all  $i, j$ , we see that the non-zero requirement is trivially satisfied in this space. Hence, focusing our attention on the RHS of the tensor product, we require for *at least* a single pair of indices  $i, j$  that

$$\sum_{r=0}^R \sum_{ln=0}^{d-1} \left( K_{ki}^{(r)} K_{nj}^{(r)\dagger} - K_{ki}^{(r')} K_{nj}^{(r')\dagger} \right) \neq 0. \quad (47)$$



On the other hand, if the two channels have different Kraus rank,  $R + 1$ ,  $R' + 1$ , then we require

$$\sum_{r=0}^R \sum_{ijln=0}^{d-1} |i\rangle \langle j| \otimes K_{ki}^{(r)} K_{nj}^{(r)\dagger} |k\rangle \langle n| - \sum_{r=0}^{R'} \sum_{ijln=0}^{d-1} |i\rangle \langle j| \otimes K_{ki}^{r'(r)} K_{nj}^{r'(r)\dagger} |k\rangle \langle n| \neq 0, \quad (48)$$

$$\implies \sum_{ij=0}^{d-1} |i\rangle \langle j| \otimes \left( \sum_{r=0}^R \sum_{kn=0}^{d-1} K_{ki}^{(r)} K_{jn}^{(r)\dagger} |k\rangle \langle n| - \sum_{r=0}^{R'} \sum_{kn=0}^{d-1} K_{ki}^{r'(r)} K_{jn}^{r'(r)\dagger} |k\rangle \langle n| \right) \neq 0, \quad (49)$$

which by reordering the indices, simplifies to

$$\sum_{ij=0}^{d-1} |i\rangle \langle j| \otimes \sum_{kn=0}^{d-1} |k\rangle \langle n| \left( \sum_{r=0}^R K_{ki}^{(r)} K_{jn}^{(r)\dagger} - \sum_{r=0}^{R'} K_{ki}^{r'(r)} K_{jn}^{r'(r)\dagger} \right) \neq 0. \quad (50)$$

With the same reasoning as above, we focus our attention to the right-hand side of the tensor product,

$$\sum_{kn=0}^{d-1} |k\rangle \langle n| \left( \sum_{r=0}^R K_{ki}^{(r)} K_{jn}^{(r)\dagger} - \sum_{r=0}^{R'} K_{ki}^{r'(r)} K_{jn}^{r'(r)\dagger} \right) \neq 0_D, \quad (51)$$

since the left-hand side is again trivially satisfying the non-zero condition. In this form, it is clear that the condition is satisfied if for a single set of indices,  $i, j, k, l$ , we have that

$$\sum_{r=0}^R K_{ki}^{(r)} K_{jn}^{(r)\dagger} - \sum_{r=0}^{R'} K_{ki}^{r'(r)} K_{jn}^{r'(r)\dagger} \neq 0. \quad (52)$$

## C Gauge Freedoms Interpreted in the Kraus Representation

To understand how the action of any spoofer (either Type-I or Type-II),  $\mathcal{E}'$ , affects the channel in more physical terms, consider the Kraus representation of  $\mathcal{E}'$ . To change representation, consider the eigenvalue decomposition of  $J_{\mathcal{E}'}$ ,

$$J_{\mathcal{E}'} = \sum_j J'_j |e_j\rangle \langle e_j|. \quad (53)$$

Using the spectral theorem, we may express the eigenvectors,  $|e_j\rangle$ , as

$$|e_j\rangle = (K'_j \otimes \mathbb{1}) |\Omega\rangle, \quad (54)$$

where  $|\Omega\rangle = \sum_k |kk\rangle$  is the un-normalised maximally entangled state. In order to extract the Kraus operator from our eigenvector, we can apply a computational basis decomposition,

$$|e_j\rangle = \sum_{il} c_{il}^j |il\rangle, \quad (55)$$

from which we see that

$$\langle il|e_j\rangle = c_{il}^j = \langle il|(K'_j \otimes \mathbb{1})|\Omega\rangle = \langle il|K'_j|l\rangle. \quad (56)$$

Since the Choi matrix,  $J_{\mathcal{E}'}$ , is known (being the output of a spoofing process), its eigenvectors in the computational basis are known, thus this quantity can be evaluated.

## D Reducing Kraus Rank via Linear Matrix Inequality

Let  $\{A_j\}_{j=1}^N$  be a set of sparse matrices whose non-zero entries correspond to the positions in the Choi matrix that are gauge freedoms w.r.t to the compatible measurement set (for either type of spoofer, see Fig. 5 for a Pauli channel example). Then we may decrease the rank of the spoofing channel by solving

$$\begin{aligned} \max_{\beta} (c \cdot \beta) \quad \text{such that} \\ J_{\mathcal{E}} + \sum_j \beta_j A_j \geq 0, \end{aligned} \tag{57}$$

where  $\beta_j \in \mathbb{R}^N$  are our variational parameters and  $c \in \mathbb{R}^N$  is an arbitrary vector. The reasoning behind this formulation is that the space of positive semi-definite matrices  $M \geq 0$  forms a cone,  $\mathcal{C}$  (cf. conic programming), with respect to a variation of each entry of the matrix. The boundary of the cone,  $\partial\mathcal{C}$  is obtained by saturating the inequality, i.e.,  $M = 0$ , which occurs when the matrix becomes singular. In other words, at the boundary  $\partial\mathcal{C}$ , one of the eigenvalues of the matrix goes to 0. Thus if we want to lower the rank of a matrix  $M$ , we can simply pick an arbitrary direction,  $c \in \mathbb{R}^N$  and vary  $\beta$  until we hit the boundary  $\partial\mathcal{C}$ . There is a caveat to this method – choices of  $c$  are better than others; with the worst choice being parallel to the main axis of the cone. However, in practise, sampling  $c$  at random makes this outcome measure 0.

By varying  $\beta$ , we can find a new Choi matrix,

$$J_{\mathcal{E}'} = J_{\mathcal{E}} + \sum_j \beta_j A_j \tag{58}$$

which, if the LMI converges, will have a rank one lower than the original channel  $J_{\mathcal{E}}$ . In order to lower the rank by more than one, we can define a recursive LMI on the sub-matrix,  $M$  spanned by the eigenvectors of  $J_{\mathcal{E}'}$  that have non-zero eigenvalues. This effectively removes the row and column corresponding to the eigenvector with a zero eigenvalue. Armed with this sub-matrix, we can simply repeat the LMI outlined in Eq. (57) with  $J_{\mathcal{E}} \leftarrow M$ , and  $\beta, c \in \mathbb{R}^{N-1}$ . To regenerate the sparse sub-matrices, notice that the gauge freedoms in the sub-matrix,  $M$ , are identical to  $\{A_j\}_{j=1}^N$  but with the same corresponding row and column removed. As such we apply the same sub-matrix generation procedure to the set  $\{A_j\}$ . This will give rise to a zero matrix for a particular value of  $j$  (a row and column will be removed that has all the non-zero indices in it), which can be removed since it makes no contribution to the LMI, giving a new, smaller set,  $\{A_j\}_{j=1}^{N-1}$ .